

Research Article

High Gain Superstrate Loaded Membrane Antenna Based on Substrate Integrated Waveguide Technology

Hamsakutty Vettikalladi

Department of Electrical Engineering, King Saud University, P.O. Box 800, Riyadh 11421, Saudi Arabia

Correspondence should be addressed to Hamsakutty Vettikalladi; hvettikalladi@ksu.edu.sa

Received 10 December 2014; Accepted 16 February 2015

Academic Editor: Chih-Hua Chang

Copyright © 2015 Hamsakutty Vettikalladi. This is an open access article distributed under the Creative Commons Attribution License, which permits unrestricted use, distribution, and reproduction in any medium, provided the original work is properly cited.

The design and the results of a single slot coupled substrate integrated waveguide (SIW) fed membrane antenna loaded with a superstrate layer are presented for 94 GHz communication system. The membrane antenna is designed using ANSYS HFSS and consists of 6 layers. The microstrip patch antenna (MPA) placed on the top pyralux substrate layer is excited by means of a longitudinal rectangular slot placed over the SIW structure in the bottom pyralux substrate. The simulated antenna impedance bandwidth is found to be 5 GHz (91.5–96.5 GHz) with a gain of 7 dBi. In order to improve the gain a superstrate layer is added above the membrane antenna. The maximum gain achieved is 14.4 dBi with an efficiency of 77.6% at 94 GHz. The results are verified using CST Microwave Studio and are found to be in good agreement.

1. Introduction

During the last decade significant advances in millimeter wave technologies have been made to cope with the increasing interest. The millimeter-wave (mmW) technology has gained a lot of attention in recent years. The W-band (75–110 GHz) window centered at 94 GHz is in focus due to its unique property of high transmission through atmospheric barriers like smoke, thin dielectrics, and clouds [1] as well as for the development of high resolution imaging applications and ultra broadband wireless communications [2]. Furthermore, the shorter wavelength at mmW permits the production of compact systems for various advance communication systems such as remote sensing, radio astronomy, cloud radar, automotive collision warning, and multi gigabits per second point to point communications.

The general requirements for mmW antennas concerns wide/ultrawide impedance bandwidth, high radiation efficiency, high gains, and compatibility with other RF communications modules. One of the suitable technologies for mmW antennas is substrate integrated circuits (SICs) [3–5]. In principle the SICs are used to synthesize and convert non-planar structures and 3D geometries into planar form which

makes SICs very attractive for millimeter wave applications [6]. Any nonplanar structure can be converted to its equivalent planar structure utilizing SICs technologies such as substrate integrated waveguide (SIW) [2]. The substrate integrated waveguide (SIW) [3–5] is the most matured and popular structure in family of SICs. Several advantages of a rectangular waveguide such as high power handling, high Q-factor, and electrical shielding are attained in SIW technology. Furthermore, the radiation leakage can be ignored in the SIW structures having metallic via placed in close proximity, resulting in propagation characteristics similar to metallic rectangular waveguides [7]. The SIW based structures can be implemented by various manufacturing processes such as conventional printed circuit board process (PCB) [8, 9], multilayer PCB process [10], photoimageable thick film technology [11], and low-temperature cofired ceramic (LTCC) technique. There are many techniques to improve the gain, either by using large arrays [12, 13], which in turn increases losses from the feed network especially at the high frequencies, or by using superstrates [14, 15]. This technique is simple and efficient to improve the gain.

In this paper we present the design and the results of a superstrate loaded multilayer membrane antenna based on

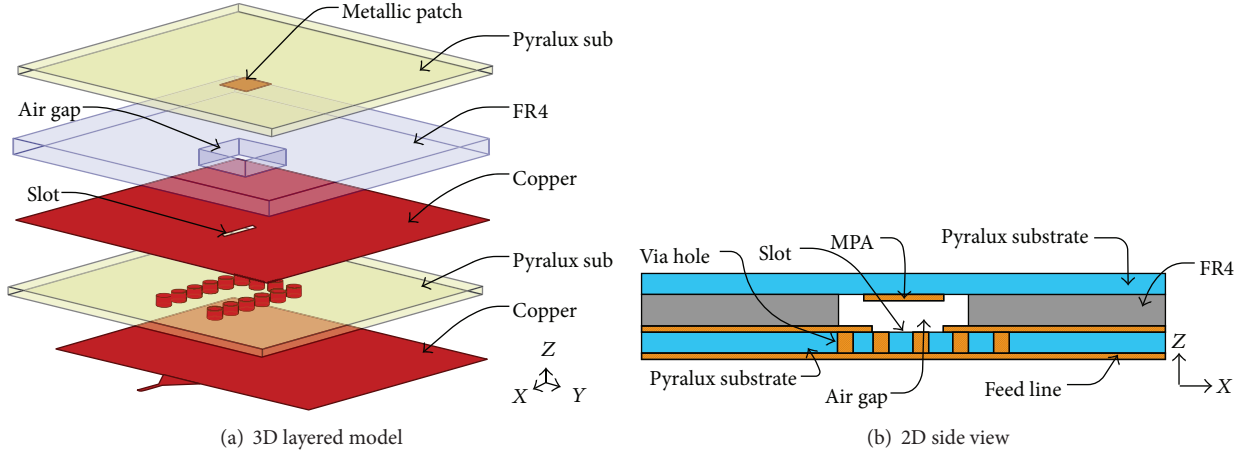


FIGURE 1: Proposed membrane antenna geometry.

SIW technology operating at 94 GHz. The available low cost, low loss DuPont pyralux TK185018R, and FR4 substrates are utilized in the proposed membrane base antenna structure and a high permittivity RT-duroid 6010ML substrate for the superstrate material. The ANSYS HFSS is utilized for modelling and the optimization of proposed antenna, whereas CST Microwave studio is used for validation of the results.

2. SIW Fed Base Membrane Antenna

2.1. Design and Configuration. The single element SIW based structure of the proposed membrane antenna with 6 layers is shown in Figure 1. The two substrates are utilized in design, that is, pyralux substrate with $\epsilon_r = 2.4$ and loss tangent ($\tan \delta$) = 0.002 and FR4 substrates with $\epsilon_r = 4.4$ and loss tangent ($\tan \delta$) = 0.02. The losses are incorporated in simulation. As shown in Figure 1(a) the top layer consists of a microstrip patch antenna (MPA) etched below the pyralux substrate. The second layer consists of the FR-4 substrate with an air cavity to support the top substrate layer. An air gap is drilled on the second layer to enhance the bandwidth of the antenna. We used the FR4 substrate because it is very cheap, low in loss, and compatible with mass production PCB technology electronics. The bottom three layers makes up a SIW slot antenna, where rectangular slot [16] in the top metallic layer of SIW is utilized to excite the MPA through the air gap made within the FR4 layer. The metallic via holes are made with in the bottom layer of pyralux substrate to form the SIW structure. The proposed membrane antenna structure in XZ plane is shown in Figure 1(b) for a better understanding of various layers. All copper layers used in proposed antenna structure have thickness of $18 \mu\text{m}$, while the thickness of pyralux and FR-4 is taken to be $50 \mu\text{m}$ and $100 \mu\text{m}$, respectively.

The distance between two rows of metallic via holes along with the dielectric between them determines the cutoff frequency. The SIW design generally works in TE_{n0} mode and does not support propagation of TM modes. For the dielectric filled waveguide (DFW) with same cutoff frequency, the

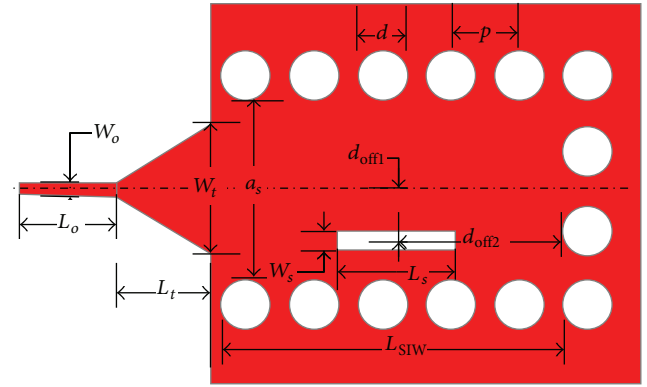


FIGURE 2: Top view of SIW antenna along with rectangular slot.

broad side dimension of waveguide, that is, a_d , is found by [17]

$$a_d = \frac{a}{\sqrt{\epsilon_r}}, \quad (1)$$

where ϵ_r is the dielectric constant of substrate and dimensions of “ a ” are taken from the standard WR-10 waveguide (i.e., 2.54 mm). Once the dimension a_d for DFW is known, we can use the following equation to find the separation distance, that is, a_s , between the via rows of SIW [18]:

$$a_s = a_d + \frac{d^2}{0.95p}, \quad (2)$$

where d is the diameter of metallic via holes connecting the upper and lower metallic layers of the bottom pyralux substrate. The via diameter (d) is taken by $d = \lambda_g/5$ and pitch, that is, centre to centre distance between the via holes, is taken by $p < 2d$ [19].

In Figure 2 the top view of proposed membrane antenna along with longitudinal slot placed on the top ground plane of SIW structure is shown. Usually the distance from the short circuited end of SIW to the centre of slot, that is, $d_{\text{off}2}$, is

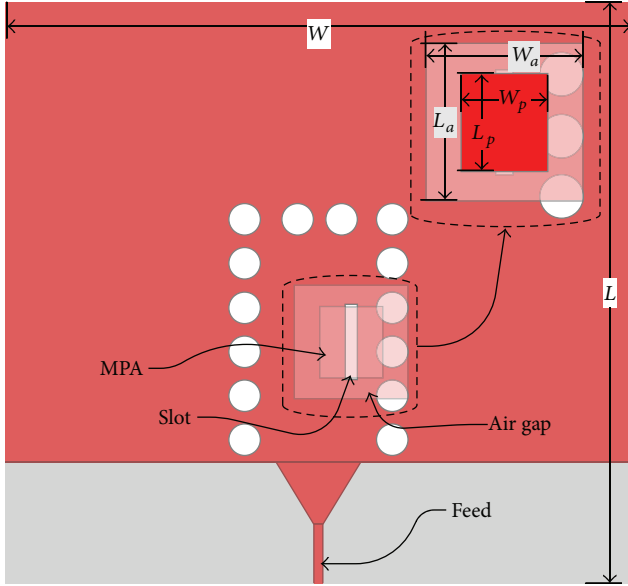


FIGURE 3: Top view of proposed membrane antenna geometry.

a quarter or odd multiple of quarter of the guided wavelength. Initially, this distance is chosen to be three quarter of the guided. Furthermore, the slot offset, that is, $d_{\text{off}1}$, is optimized for proper excitation of longitudinal slot as well as the metallic patch antenna on the top layer. The initial dimension for longitudinal slot length is taken by [17]

$$L_s = \frac{\lambda_o}{\sqrt{2(\epsilon_r + 1)}}. \quad (3)$$

The pyralux substrate with patch on top layer is supported by a layer of FR4 substrate having an optimized air gap of $1.8 \text{ mm} \times 1.8 \text{ mm}$ under the MPA. The optimized dimensions for MPA are found to be $1.12 \times 0.99 \text{ mm}$. The total size of antenna is found to be $10 \text{ mm} \times 10 \text{ mm}$. A conventional 50Ω microstrip line is utilized as a feed element in the proposed antenna. The microstrip to SIW transition consisting of a tapered microstrip is also optimized for proper impedance matching. The detailed view of proposed single membrane antenna along with various important design parameters for MPA and air gap in FR-4 substrate are well explained in [20] and in Figure 3.

The optimum dimension for the proposed membrane antenna structure is $W_o = 0.145 \text{ mm}$, $W_t = 1.34 \text{ mm}$, $L_o = 1 \text{ mm}$, $L_t = 0.9 \text{ mm}$, $d = 0.5 \text{ mm}$, $p = 0.7 \text{ mm}$, $a_s = 1.5 \text{ mm}$, $W_s = 0.2 \text{ mm}$, $L_s = 1.225 \text{ mm}$, $L = 3.5 \text{ mm}$, $d_{\text{off}1} = 0.55 \text{ mm}$, $d_{\text{off}2} = 1.4125 \text{ mm}$, $L_a = 1.85 \text{ mm}$, $W_a = 1.85 \text{ mm}$, $L_p = 1.15 \text{ mm}$, $W_p = 1.05 \text{ mm}$, $L = 10 \text{ mm}$, and $W = 10 \text{ mm}$.

2.2. Results and Discussion. The proposed antenna structure is simulated and optimized using ANSYS High Frequency Structure Simulator (HFSS[®]). The results are further verified by simulating the proposed antenna structure in CST Microwave Studio.

A comparison between the simulation results of S_{11} and gain obtained from HFSS and CST are given in Figure 4.

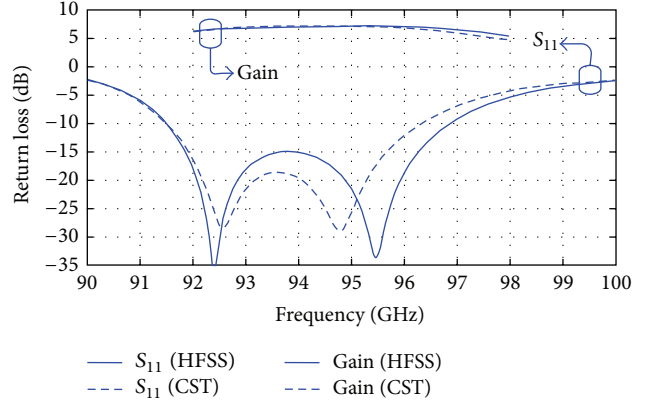


FIGURE 4: Simulated return loss S_{11} and realized gain.

The two resonances at 92.4 GHz and 95.5 GHz are due to presence of slot and patch in antenna geometry, respectively, which are kept in close proximity to achieve wide impedance bandwidth. The FR-4 support with air gap plays an important role in merging the two resonances to achieve a wide impedance bandwidth. The antenna impedance bandwidth is found to be 5.4 GHz (91.5–96.9 GHz) from HFSS while from CST the impedance bandwidth is found to be approximately 4.9 GHz (91.5–96.4 GHz). The gain is found to be 7 dBi at the center frequency of 94 GHz. The peak gain of 7.5 dB is found at 95.5 GHz. Furthermore, the antenna gain remains above 6.7 dB in whole frequency band of operation.

The antenna radiation pattern in both E-plane (horizontal plane) and H-plane (vertical plane) remains similar throughout the whole frequency band of operation. The comparison of 2D radiation patterns obtained from HFSS and CST at 92, 94, and 96 GHz in both vertical plane ($\varphi = 90^\circ$) and horizontal plane ($\varphi = 0^\circ$) plane is shown in Figures 5 and 6, respectively. By increasing the ground plane size the small ripples in E-plane radiation pattern can be reduced, which are mainly due to diffraction of the limited ground plane. The cross polarization ratio of less than -20 dB is achieved in E- and H-plane radiation patterns, respectively. The antenna 3 dB beam width is found to be 50° and 45° in E- and H-plane, respectively.

From the above results, it is noted that the peak gain obtained is only 7.5 dBi which is not enough for the point to point communication at 94 GHz. So we added a superstrate layer to improve the gain.

3. Improvement of Gain with Superstrate Layer

Side view of proposed antenna with superstrate layer is shown in Figure 7. It consists of the base antenna as explained in Section 2 and a dielectric superstrate layer is added above it. The material used for the superstrate is Roger RT-duroid 6010ML ($\epsilon_r = 10.2$, and $\tan(\delta) = 0.003$). A Rohacell foam layer of permittivity 1.05 is sandwiched between base antenna and superstrate as a support. The thickness t , dimension S ,

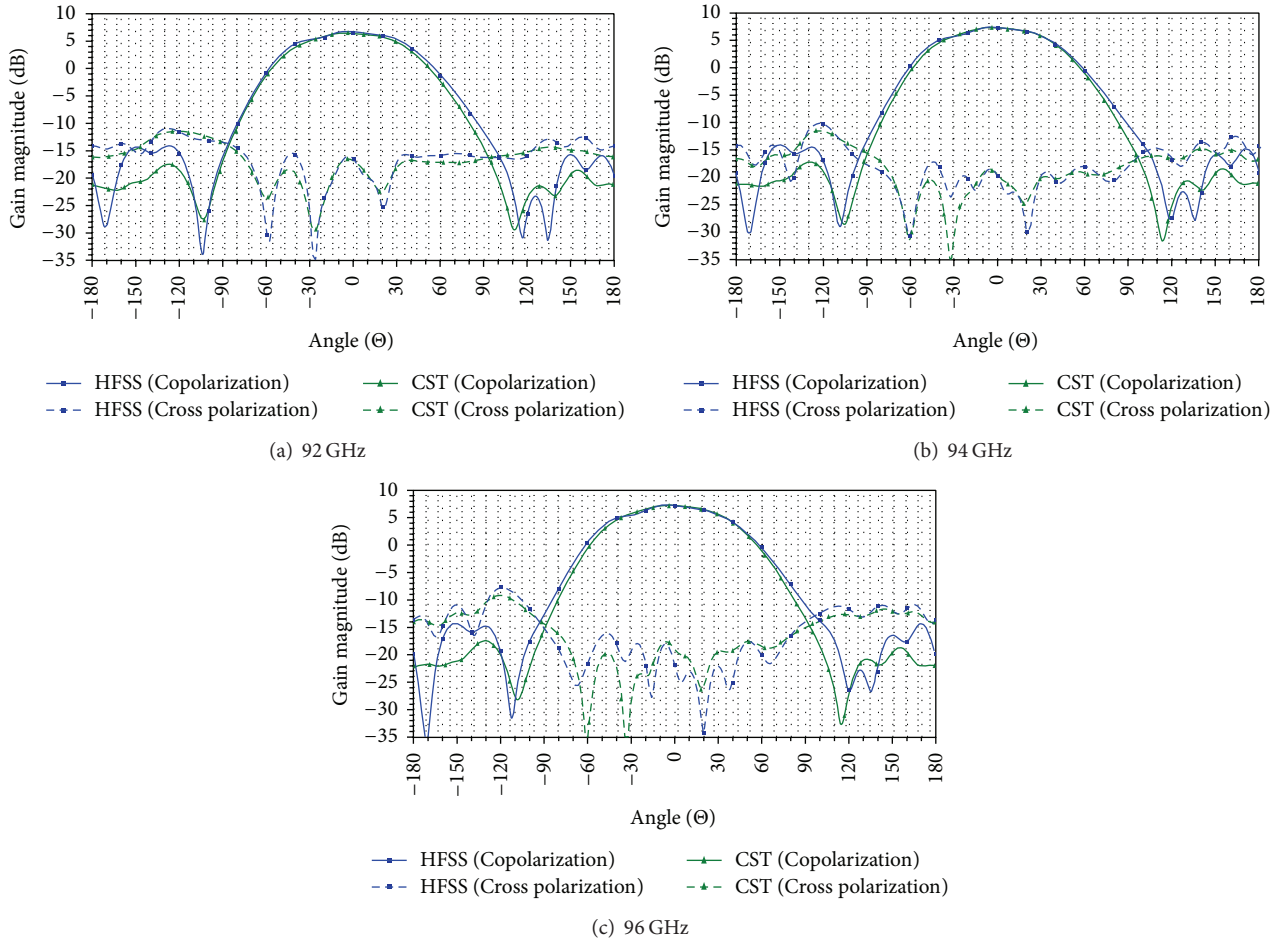


FIGURE 5: 2D radiation pattern in H-plane with co- and cross polarization.

and the height of the superstrate h are studied and optimised as explained below.

The variation of S_{11} and gain with different superstrate thickness ($t = 0.127, 0.254, \text{ and } 0.635 \text{ mm}$) with a constant height of $h = 0.55\lambda_0$ and size $S = 3.125 \times 3.125\lambda_0 = 10 \times 10 \text{ mm}^2$ is shown in Figure 8. It is noted that even though the maximum gain is achieved for a superstrate thickness of $t = 0.635$ as compared to $t = 0.127\lambda_0$, the side lobe level (SLL) is worst as investigated in Figure 9. This poor SLL with large thickness of the material may be due to the surface waves at this high frequency. Hence we took the commercially available thickness $t = 0.127 \text{ mm}$ as the superstrate material. The side lobe levels in this case are less than -15 dB in the whole frequency band of interest.

Figure 10 shows the variation of return loss (S_{11}) and gain for different superstrate heights, $h = 0.5\lambda_0, 0.55\lambda_0, 0.6\lambda_0$, respectively, with a superstrate size of $S = 3.125 \times 3.125\lambda_0$. It is clear from the figure that the maximum gain with worst bandwidth is achieved for a superstrate height of $h = 0.55\lambda_0$, while for the good desired bandwidth of $92 \text{ GHz} - 96 \text{ GHz}$ is achieved with a height of $h = 0.6\lambda_0$ and is the best one. The high gain at $h = 0.55\lambda_0$ is because of the narrow bandwidth. We took the height $h = 0.6\lambda_0$ for the next optimisation simulation.

The variation of the superstrate size S for an optimised height of $h = 0.6\lambda_0$ is studied as shown in Figure 11. It is clear that the maximum gain of 14.4 dBi with good bandwidth of $92 \text{ GHz} - 96 \text{ GHz}$ is achieved for a superstrate size of $S = 2\lambda_0 \times 2\lambda_0$.

The comparison of CST and HFSS results of return loss (S_{11}), gain, and directivity of the optimised dimension is given in Figure 12. The $2:1$ VSWR bandwidth is noted to be $92 \text{ GHz} - 96 \text{ GHz}$ (i.e., 4.25% impedance bandwidth) with a maximum gain of 14.4 dBi and a directivity of 15.5 dBi at 94 GHz , hence a radiation efficiency of 77.6% . The results are in a good agreement between the CST and HFSS simulations. There is a gain enhancement of 7.2 dBi with the loaded superstrate layer as compared to without superstrate.

The E-plane and H-plane radiation characteristics by using CST and HFSS simulations are shown in Figures 13(a) and 13(b), respectively. The simulated results for the frequencies at 92 GHz , 94 GHz , and 96 GHz , respectively, are presented. Both simulation results are in good agreement. E-plane has the side lobe of level -14.8 dB and 3 dB beam width of 27.9° at 94 GHz . The H-plane has the side lobe of level -22.1 dB and 3 dB beam width of 25.1° at the same frequency. There is a cross polar level of less than -25 dB at all frequencies in both planes.

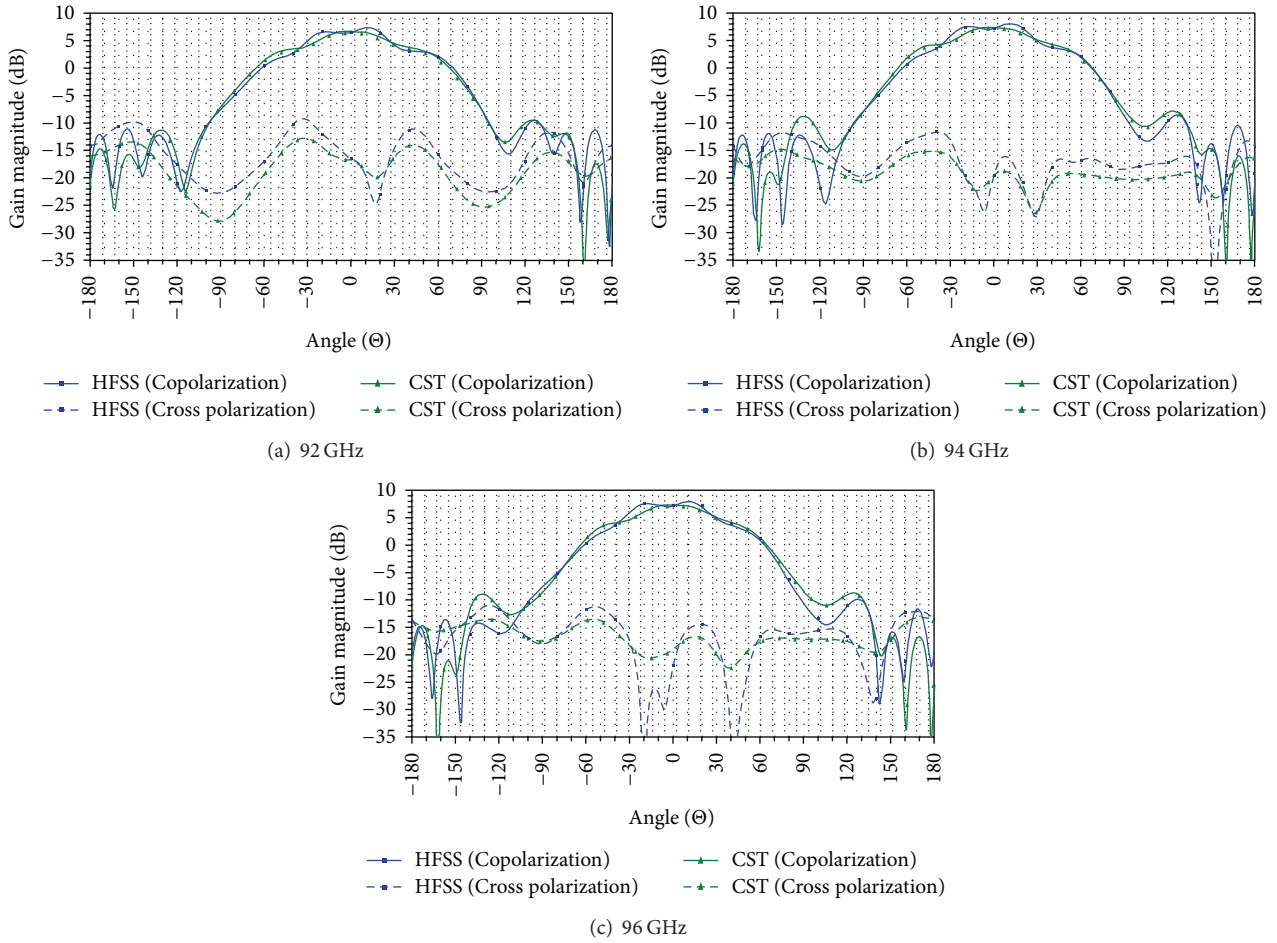


FIGURE 6: 2D radiation pattern in E-plane with co- and cross polarization.

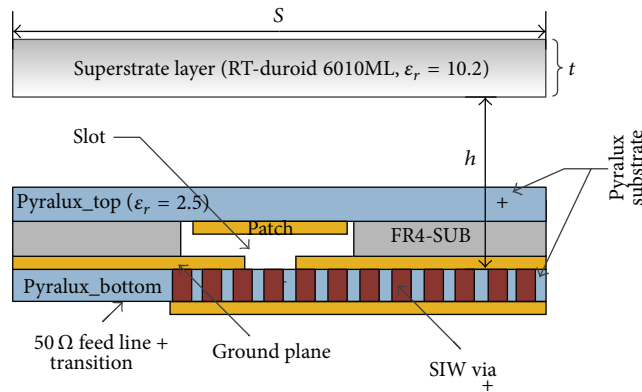


FIGURE 7: Cutting plane of a membrane antenna with superstrate layer, ground plane size $10 \times 10 \text{ mm}^2$.

4. Conclusion

The design and the results of a superstrate loaded membrane antenna based on SIW technology are presented. A microstrip patch antenna along with a longitudinal slot is utilized to achieve a wide impedance bandwidth of 5 GHz at centre frequency of 94 GHz. The gain of the antenna for

the single element is found to be above 6.5 dB in whole frequency band of operation and is further improved to a maximum of 14.4 dBi with an addition of superstrate layer. Furthermore, similar antenna radiation patterns are achieved in whole frequency band of operation. The proposed antenna finds applications in 94 GHz point-point communication systems.

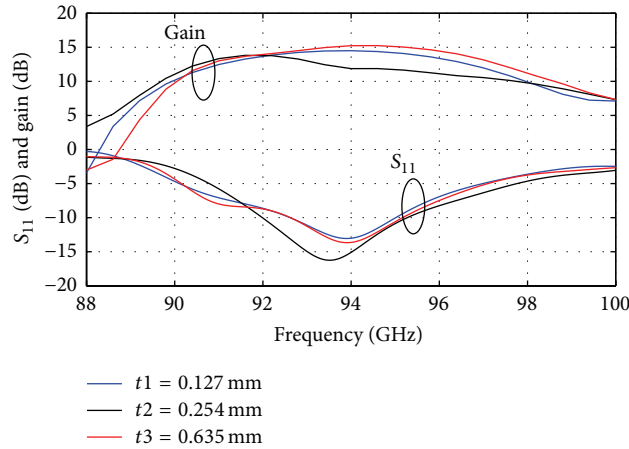


FIGURE 8: Simulated results of S_{11} and gain with various superstrate thickness for a fixed height $h = 0.55\lambda_0$, and size of the superstrate $S = 3.125 \times 3.125\lambda_0$.

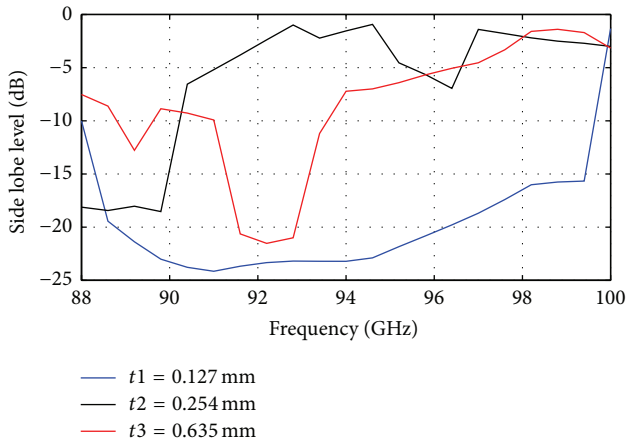


FIGURE 9: The variation of side lobe level of the antenna with the variation of the thickness of the superstrate.

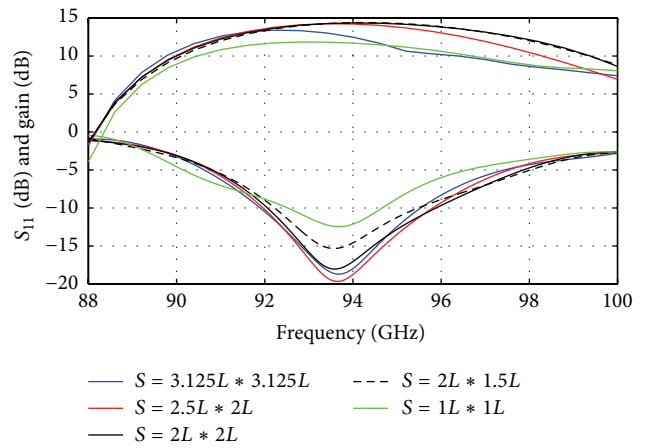


FIGURE 11: Variation of S_{11} and gain for different dimensions size S with a fixed superstrate height of $h = 0.6\lambda_0$.

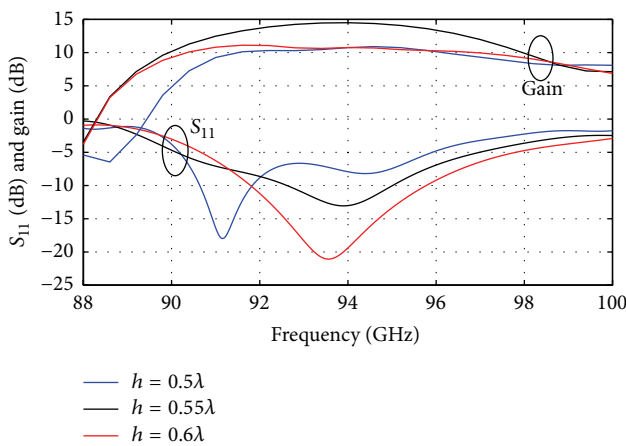


FIGURE 10: Variation of S_{11} and gain with a superstrate dimension of $S = 3.125 \times 3.125\lambda_0$, and with different heights of $h = 0.5\lambda_0$, $h = 0.55\lambda_0$, and $h = 0.6\lambda_0$.

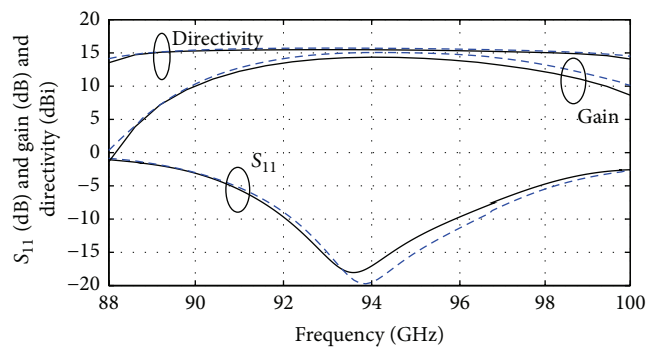


FIGURE 12: Results of S_{11} , gain, and directivity over frequency with an optimised superstrate dimension $S = 2 \times 2\lambda_0$, an optimised height $h = 0.6\lambda_0$, and an optimised thickness $t = 0.127$ mm.

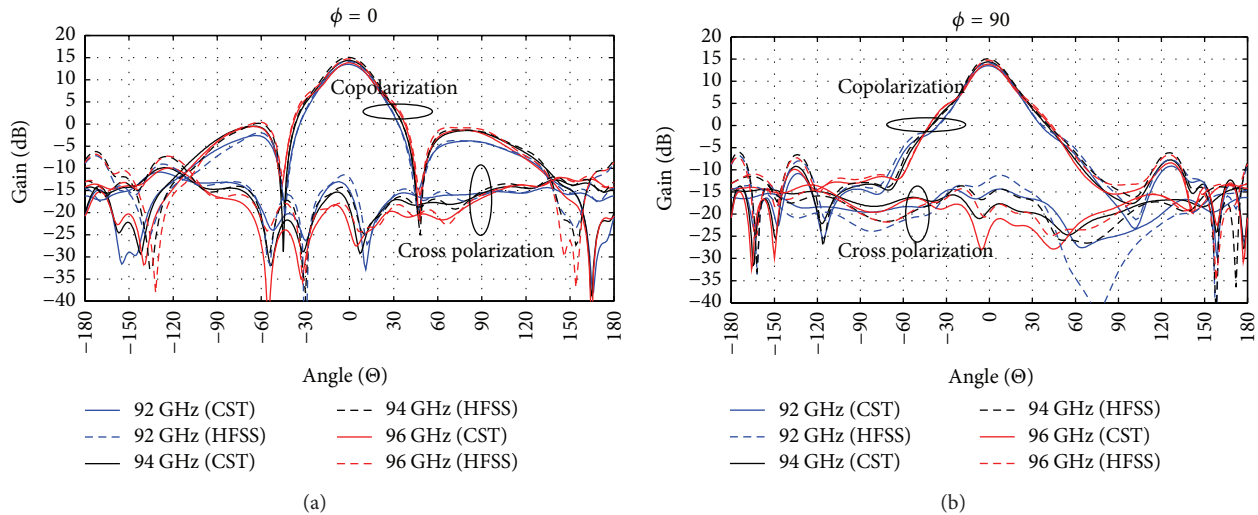


FIGURE 13: Simulated (a) E-plane and (b) H-plane radiation characteristics of superstrate antenna for an optimised superstrate dimension $S = 2\lambda_0 \times 2\lambda_0$, height $h = 0.6\lambda_0$, and thickness $t = 0.127$ mm.

Conflict of Interests

The author declares that there is no conflict of interests regarding the publication of this paper.

Acknowledgment

The author would like to thank the Deanship of Scientific Research, Research Center at College of Engineering, King Saud University, for funding this research work.

References

- [1] E. S. Roseblum, "Atmosphere absorption of 10-400 KMQS radiation: summary and biography up to 1961," *Microwave Journal*, vol. 4, pp. 91-96, 1961.
- [2] K. Wu, Y. J. Cheng, T. Djeraji, and W. Hong, "Substrate-integrated millimeter-wave and terahertz antenna technology," *Proceedings of the IEEE*, vol. 100, no. 7, pp. 2219-2232, 2012.
- [3] J. Hirokawa and M. Ando, "Single-layer feed waveguide consisting of posts for plane tem wave excitation in parallel plates," *IEEE Transactions on Antennas and Propagation*, vol. 46, no. 5, pp. 625-630, 1998.
- [4] D. Deslandes and K. Wu, "Single-substrate integration technique of planar circuits and waveguide filters," *IEEE Transactions on Microwave Theory and Techniques*, vol. 51, no. 2, pp. 593-596, 2003.
- [5] D. Deslandes and K. Wu, "Accurate modeling, wave mechanisms, and design considerations of a substrate integrated waveguide," *IEEE Transactions on Microwave Theory and Techniques*, vol. 54, no. 6, pp. 2516-2526, 2006.
- [6] K. Wu, D. Deslandes, and Y. Cassivi, "The substrate integrated circuits—a new concept for high frequency electronics and optoelectronics," in *Proceedings of the 6th International Conference on Telecommunications in Modern Satellite, Cable and Broadcasting Service (TELSIKS '03)*, vol. 1, pp. 3-5, October 2003.
- [7] M. Bozzi, A. Georgiadis, and K. Wu, "Review of substrate-integrated waveguide circuits and antennas," *IET Microwaves, Antennas and Propagation*, vol. 5, no. 8, pp. 909-920, 2011.
- [8] L. Yan, W. Hong, G. Hua, J. Chen, K. Wu, and T. J. Cui, "Simulation and experiment on SIW slot array antennas," *IEEE Microwave and Wireless Components Letters*, vol. 14, no. 9, pp. 446-448, 2004.
- [9] W. Hong, B. Liu, G. Q. Luo et al., "Integrated microwave and millimeter wave antennas based on SIW and HMSIW technology," in *Proceedings of the IEEE International Workshop on Antenna Technology: Small and Smart Antennas Metamaterials and Applications (iWAT '07)*, pp. 69-72, March 2007.
- [10] H. Nakano, R. Suga, Y. Hirachi, J. Hirokawa, and M. Ando, "60 GHz post-wall waveguide aperture antenna with directors made by multilayer PCB process," in *Proceedings of the 5th European Conference on Antennas and Propagation (EUCAP '11)*, pp. 3113-3116, Rome, Italy, April 2011.
- [11] D. Stephens, P. R. Young, and I. D. Robertson, "W-band substrate integrated waveguide slot antenna," *Electronics Letters*, vol. 41, no. 4, pp. 165-167, 2005.
- [12] S.-S. Oh, J. Heo, D.-H. Kim, J.-W. Lee, M.-S. Song, and Y.-S. Kim, "Broadband millimeter-wave planar antenna array with a waveguide and microstrip-feed network," *Microwave and Optical Technology Letters*, vol. 42, no. 4, pp. 283-287, 2004.
- [13] J. Navarro, "Wide-band, low-profile millimeter-wave antenna array," *Microwave and Optical Technology Letters*, vol. 34, no. 4, pp. 253-255, 2002.
- [14] S. M. Meriah, E. Cambiaggio, R. Staraj, and F. T. Bendimerad, "Gain enhancement for microstrip reflectarray using superstrate layer," *Microwave and Optical Technology Letters*, vol. 46, no. 2, pp. 152-154, 2005.
- [15] H. Vettikalladi, O. Lafond, and M. Himdi, "High-efficient and high-gain superstrate antenna for 60-GHz indoor communication," *IEEE Antennas and Wireless Propagation Letters*, vol. 8, pp. 1422-1425, 2009.
- [16] W. M. Abdel-Wahab and S. Safavi-Naeini, "Wide-bandwidth 60-GHz aperture-coupled microstrip patch antennas (MPAs) fed by substrate integrated waveguide (SIW)," *IEEE Antennas and Wireless Propagation Letters*, vol. 10, pp. 1003-1005, 2011.

- [17] S. Moitra, A. Kumar Mukhopadhyay, and A. Kumar Bhattacharjee, "Ku-Band substrate integrated waveguide (SIW) slot array antenna for next generation networks," *Global Journal of Computer Science and Technology Network, Web & Security*, vol. 13, no. 5, 2013.
- [18] Y. Cassivi, L. Perregrini, P. Arcioni, M. Bressan, K. Wu, and G. Conciauro, "Dispersion characteristics of substrate integrated rectangular waveguide," *IEEE Microwave and Wireless Components Letters*, vol. 12, no. 9, pp. 333–335, 2002.
- [19] K. Wu, D. Deslandes, and Y. Cassivi, "The substrate integrated circuits—a new concept for high-frequency electronics and optoelectronics," in *Proceedings of the 6th International Conference on Telecommunications in Modern Satellites, Cable and Broadcasting Services (TELSIKS '03)*, Niš, Serbia, October 2003.
- [20] H. Vettikalladi, M. K. Saleem, and M. A. S. Alkanhal, "Millimeter wave antenna based on substrate integrated waveguide for 94 GHz communication systems," in *Proceedings of the International Workshop on Antenna Technology (iWAT '14)*, Sydney, Australia, March 2014.

